$Ce_{1-x}Rh_xO_{2-\delta}$ Solid Solution Formation in Combustion-Synthesized Rh/CeO_2 Catalyst Studied by XRD, TEM, XPS, and EXAFS

Arup Gayen,[†] K. R. Priolkar,[‡] P. R. Sarode,[‡] V. Jayaram,[†] M. S. Hegde,*[,†] G. N. Subbanna,[§,||] and S. Emura[⊥]

Solid State and Structural Chemistry Unit and Materials Research Centre, Indian Institute of Science, Bangalore-560012, India, Department of Physics, Goa University, Goa-403206, India, and Institute of Scientific and Industrial Research, Osaka University, Mihoga-oka 8-1, Ibaraki, Osaka, 567-0047, Japan

Received February 16, 2004. Revised Manuscript Received March 23, 2004

Ionically dispersed Rh over CeO_2 in Rh/CeO_2 catalysts prepared by a single step solution combustion method is shown to improve the redox property and catalytic activity. The H_2/Rh ratio obtained from hydrogen uptake measurement was 5.4, 2.4, and 2.1, respectively in 0.5, 1, and 2% Rh/CeO_2, indicating a significant contribution from the reduction of CeO_2 in the presence of Rh. In 1% Rh/CeO_2, the light-off temperature for CO oxidation is about 80 °C lower compared to Rh metal and 190 °C lower than that of Rh_2O_3. The enhanced redox property and CO oxidation activity of the catalyst has been correlated with the structure. The X-ray diffraction (XRD) pattern could be refined to the fluorite structure with Rh substituting in the Ce site. Transmission electron microscopy (TEM) images show only CeO_2 crystallites of about 50 nm and no evidence of any metal particles up to 1 atom % Rh. X-ray photoelectron spectroscopy (XPS) studies demonstrate that Rh is dispersed in the +3 oxidation state on CeO_2 with enhanced Rh ion concentration in the surface layers. An average coordination number of 2.5 at a distance of 2.05 Å in the first shell is obtained around Rh ions from extended X-ray absorption fine structure (EXAFS) spectroscopy, indicating an oxide ion vacancy around the Rh ion. The correlations at 2.72 and 3.16 Å correspond to Rh−Rh and Rh−Ce interactions, respectively. Thus, the enhanced catalytic activity of Rh/CeO_2 is shown to be due to the formation of a $Ce_{1-x}Rh_xO_{2-\delta}$ type of solid solution with $-\square-Rh^{3+}-O-Ce^{4+}-$ kind of linkages on the surface.

Introduction

Rhodium dispersed over an oxide support has been well-recognized for its high activity toward NO reduction as well as CO oxidation.[1−4] Understanding the Rh−support interaction is important in the broad area of automotive exhaust catalysis.[5] Usually CeO_2 is impregnated over Al_2O_3 and on such an oxide support Rh metal/oxide is impregnated. The Rh/Al_2O_3 interaction can be quite different from that of Rh/CeO_2 because CeO_2 is more ionic and also it is reducible. In the case of Rh/Al_2O_3 catalysts, a metal−support interaction has been shown to be present between zerovalent Rh atoms at the interface and oxygen ions of the support.[6] An EXAFS study on 5 wt % $Rh/Ce_{0.5}Zr_{0.5}O_2$ catalyst indicates that Rh metal particles are dispersed on the oxide support, which can get oxidized to Rh oxide clusters in the presence of NO + CO.[7] Fajardie et al. have shown that in the 0.3 wt % Rh/CeO_2-ZrO_2 system, the catalytic activity is due to Rh^{x+} species stabilized with two oxygen vacancies of the reduced CeO_2-ZrO_2 support.[8] Ce L_3 EXAFS has been used to monitor the redox process on impregnated Rh/CeO_2 by Fallah et al.[9] Their study shows a faster dissociation of hydrogen attributed to the presence of metallic rhodium on the ceria support. Generally, 0.5−1 wt % Rh, together with Pd and Pt added to the oxide support, makes an active three-way catalyst (TWC).[10] Dispersion of the noble metal component in ionic form over CeO_2 nanocrystallites can be an effective method to disperse Rh so that more Rh atom/

* Corresponding author. Fax: +91-80-23601310. E-mail: mshegde@sscu.iisc.ernet.in.
† Solid State and Structural Chemistry Unit, Indian Institute of Science.
‡ Goa University.
§ Deceased.
|| Materials Research Centre, Indian Institute of Science.
⊥ Osaka University.

(1) Taylor, K. C. In *Catalysis−Science and technology*; Anderson, J. R., Boudart, M., Ed.; Springer-Verlag: Berlin, 1984; p 121.
(2) Taylor, K. C. *Catal. Rev.−Sci. Eng.* **1993**, *35*, 457.
(3) Cho, B. K. *J. Catal.* **1991**, *131*, 74.
(4) Zafiris, G. S.; Gorte, R. J. *J. Catal.* **1993**, *131*, 561.
(5) Gandhi, H. S.; Graham, G. W.; McCabe, R. W. *J. Catal.* **2003**, *216*, 433.
(6) van Zon, J. B. A. D.; Koningsberger, D. C.; van't Blick, H. F. J.; Sayers, D. E. *J. Chem. Phys.* **1985**, *82*(15), 5742.
(7) Vlaic, G.; Fornasiero, P.; Martra, G.; Fonda, E.; Kašper, J.; Marchese, L.; Tomat, E.; Coluccia, S.; Graziani, M. *J. Catal.* **2000**, *190*, 182.
(8) Fajardie, F.; Tempère, J.-F.; Manoli, J.-M.; Touret, O.; Blanchard, G.; Djéga-Mariadossou, G. *J. Catal.* **1998**, *179*, 469.
(9) Fallah, J. El; Boujana, S.; Dexpert, H.; Kiennemann, A.; Majerus, J.; Touret, O.; Villain, F.; Normand, F. Le *J. Phys. Chem.* **1994**, *98*, 5522.
(10) Kašper, J.; Fornasiero, P.; Hickey, N. *Catal. Today* **2003**, *77*, 419.

10.1021/cm040126l CCC: $27.50
Published on Web 05/07/2004

Rh ion can become active sites for adsorption in contrast to Rh atoms on Rh metal particles supported on oxides. In the case of Rh metal particle, only the surface Rh atoms are accessible for adsorption. Stronger ionic interaction between Rh ion and CeO_2 can drastically reduce loss of noble metal by evaporation and sintering due to aging of the catalyst.

In recent times we have shown that ionically dispersed Cu^{2+}, Pd^{2+}, and Pt^{2+} in the form of $Ce_{1-x}M_xO_{2-\delta}$, (M = Cu, Pd, Pt) solid solution give much higher catalytic activity for CO oxidation, NO reduction, and hydrocarbon oxidation compared to the respective metal particles.[11−13] The enhancement in catalytic activity of these catalysts has been attributed to the high dispersion of metal in the form of ions due to the formation of $Ce_{1-x}M_xO_{2-\delta}$ type of solid solution primarily on the surface. To understand the PM−ceria interaction further, we have studied Rh/CeO_2 and here we report the formation of $Ce_{1-x}Rh_xO_{2-\delta}$ solid solution in combustion-synthesized 0.5−2 atom % Rh/CeO_2 catalyst. We show that rhodium ions dispersed over CeO_2 are much more active toward CO oxidation compared to Rh metal.

Experimental Section

Synthesis. The combustion mixture for the preparation of 1% Rh/CeO_2 contained $(NH_4)_2Ce(NO_3)_6$, $RhCl_3{\cdot}xH_2O$, and $C_2H_6N_4O_2$ (oxalyldihydrazide) in the mole ratio 0.99:0.01:2.376. Oxalyldihydrazide (ODH) prepared from diethyl oxalate and hydrazine hydrate was used as the fuel. A typical preparation consisted of dissolving 10 g of $(NH_4)_2Ce(NO_3)_6$ (E. Merck India Ltd., 99.9%), 4.75 mL of $RhCl_3.xH_2O$ (Arora Matthey Ltd. 40% Rh) solution containing 0.4% Rh, and 5.175 g of ODH in a minimum volume of water (∼30 cm^3) in a borosilicate dish of 130 mL capacity followed by introduction of the dish containing the redox mixture into a muffle furnace maintained at ∼350 °C. Initially the solution boiled with frothing and foaming and underwent dehydration. At the point of complete dehydration, the surface ignited, burning with a flame (∼1000 °C) and yielding a voluminous solid product within 2 min. The flame itself lasts for 10−20 s and within a time interval of 60 s the temperature falls from 1000 °C to about 350 °C. These compounds were prepared in an open muffle furnace kept in a fume cupboard with exhaust. Rh metal and Rh_2O_3 were obtained from Arora Matthey Ltd. and used as such. For comparison, 1 atom % Rh + CeO_2 and 1 atom % Rh_2O_3 + CeO_2 composite were made by physically mixing combustion-synthesized CeO_2 with fine Rh metal powder and Rh_2O_3, respectively.

Characterization. XRD patterns of the prepared catalysts and physically mixed materials were recorded on a Philips X'Pert diffractometer at a scan rate of 0.5° min^{-1} with 0.02° step size in the 2θ range 10°−90°. High-resolution XRD data for Rietveld analysis was collected on a Rigaku-2000 diffractometer with a rotating anode using Cu Kα radiation with a graphite-crystal monochromator to filter Kβ lines. Data were obtained at a scan rate of 1° min^{-1} with 0.02° step size in the 2θ range 10°−110° and the structure was refined using the FullProf-fp2k program. The number of parameters refined simultaneously was 19.

BET surface area was determined by the nitrogen adsorption−desorption method at liquid nitrogen temperature using a Quantachrome NOVA 1000 surface area analyzer. Prior to the analysis the samples were degassed for 2 h at 200 °C.

TEM study of powders of these materials was carried out using a JEOL JEM-200CX transmission electron microscope operated at 200 kV.

XPS of the samples was recorded in an ESCA-3 Mark II spectrometer (VG Scientific Ltd., England) using Al Kα radiation (1486.6 eV). Binding energies were corrected from charge effects by reference to the C(1s) peak of carbon contamination at 285 eV and measured with a precision of ±0.2 eV. For XPS analysis, the powder samples were made into pellets of 8 mm diameter employing 12 kN pressure and placed into an ultrahigh vacuum (UHV) chamber at 10^{-9} Torr housing the analyzer. The experimental data were curve fitted with Gaussian peaks after subtracting a linear background.

EXAFS Measurements. EXAFS spectra of Rh K-edge in combustion-synthesized catalysts and reference samples were recorded at room temperature in transmission mode by using synchrotron radiation, employing a Si(111) double-crystal monochromator at BL01B1 beamline at the Japan Synchrotron Radiation Research Institute (SPring-8). The monochromator was fully tuned in order to get optimal resolution. The slit width of the monochromator exit was 1.5 mm vertical and 8 mm horizontal to ensure a good signal-to-noise ratio. As the focusing mirrors used in this beamline are coated with rhodium, they were not used. During the measurement the synchrotron was operated at an energy of 8 GeV and a current between 60 and 100 mA. The spectra were scanned in the range from 22 900 to 24 200 eV for the Rh K-edge EXAFS. The photon energy was calibrated for each scan with the first inflection point of Rh K-edge in Rh metal (23 219 eV). Both the incident (I_o) and transmitted (I) synchrotron beam intensities were measured simultaneously using ionization chambers filled with a mixture of 100% Ar gas and a mixture of 50% Ar and 50% Kr gases, respectively. The absorbers were made by pressing the samples into pellets of 10 mm diameter with boron nitride as binder.

EXAFS data have been analyzed using the UWXAFS program.[14]Background subtaction and conversion to the EXAFS function, $\chi(k)$, of the X-ray absorption data was done using AUTOBK 2.61. Since $\chi(k)$ is a superposition of an unknown number of coordination shells, the Fourier transform (FT) technique was used to extract information about the individual shells. Here, FT of $\chi(k)$ to R space with k^3 weighting factor and Hanning window function (Dk1 and Dk2 = 0.1) has been performed in the 3−12 $Å^{-1}$ range, yielding a function $\Phi(R)$. The function $\Phi(R)$, where R is the distance from the absorber atom, is called a radial distribution function (RDF) or radial structure function (RSF). The value of the amplitude reduction factor (S_o^2) is deduced from Rh K-edge EXAFS of Rh metal with known crystal structural data.[15] The theoretical calculation of backscattering amplitude and phase shift functions are obtained by using the FEFF (6.01) program.[16] The input files for FEFF are directly given from crystal structure information like lattice parameters, space group, and absorbing core. The experimental EXAFS data were fitted with the theoretical EXAFS function using the FEFFIT (2.52) program.[17] E_o is one of the fitting parameters in FEFFIT. Initially, it was taken as the energy corresponding to the first inflection point in the derivative spectra of an individual compound. For Rh metal, it is found to be 23 219 eV within the error of 1 eV. After fitting, the final values of E_o obtained are 23 219.6 and 23 222.3 eV for Rh metal and Rh_2O_3, respectively. The goodness of fit has been judged by means of χ^2, reduced χ^2, and R factor, as discussed elsewhere.[18,19] From this analysis, struc-

(11) Priolkar, K. R.; Bera, P.; Sarode, P. R.; Hegde, M. S.; Emura, S.; Kumashiro, R.; Lalla, N. P. *Chem. Mater.* **2002**, *14*, 2120.
(12) Bera, P.; Priolkar, K. R.; Sarode, P. R.; Hegde, M. S.; Emura, S.; Kumashiro, R.; Lalla, N. P. *Chem. Mater.* **2002**, *14*, 3591.
(13) Bera, P.; Priolkar, K. R.; Gayen, Arup; Sarode P. R.; Hegde, M. S.; Emura, S.; Kumashiro, R.; Subanna, G. N.; Jayram, V. *Chem. Mater.* **2003**, *15*, 1049.
(14) Newville, M.; Līviņš, P.; Yacoby, Y.; Rehr, J. J.; Stern, E. A. *Phys. Rev. B* **1993**, *47*, 14126.
(15) Pearson, W. P. In *Handbook of Lattice Spacings and Structures of Metals and Alloys*; Pergamon: New York, 1958.
(16) Zabinsky, S. I.; Rehr, J. J.; Ankudinov, A.; Albers, R. C.; Eller, M. J. *Phys. Rev. B* **1995**, *52*, 2996.
(17) Stern, E. A.; Newville, M.; Ravel, B.; Yacoby, Y.; Haskel, D. *Physica B* **1995**, *208/209*, 117.
(18) Press, W. H.; Teulosky, S. A.; Vetterling, W. T.; Flannery, B. P. In *Numerical Recipies*; Cambridge University Press: New York, 1992.

tural parameters such as coordination numbers (N), bond distance (R), and Debye−Waller factor (σ) have been calculated.

H_2 Uptake Measurement. Hydrogen uptake experiments were performed in a continuous flow gradient less microreactor of length 30 and 0.4 cm internal diameter with 5.49% H_2/Ar (certified calibration gas mixture) flowing at 30 sccm at a linear heating rate of 10 °C min^{-1}. Before each measurement, the catalyst (100 mg, 40/80 mesh size diluted with 100 mg SiO_2, 30/60 mesh size) was oxidized in situ in oxygen flow at 500 °C for 3 h, followed by degassing in Ar flow to experimental temperature in order to minimize the contribution from adsorbed species. Hydrogen concentration was monitored by a thermal conducting detector (TCD) connected to a personal computer for data storage. The TCD response was quantitatively calibrated by monitoring the reduction of a known amount of CuO.

Temperature-Programmed Reaction (TPR). The catalytic reactions were carried out in a temperature-programmed reaction system equipped with a quadrupole mass spectrometer QXK300 (VG Scientific Ltd., England) for product analysis in a packed bed tubular quartz reactor of internal diameter 0.4 cm × 25 cm length at atmospheric pressure. Typically, 50 mg of Rh/CeO_2 catalyst (40/80 mesh size) diluted with SiO_2 (30/60 mesh size) was loaded in the reactor to get a column length of 1.1 cm with its ends plugged with ceramic wool. The feed (100 sccm) consisted of 2 vol % CO and 6 vol % O_2 with He as diluent gas, which gave a gas hourly space velocity (GHSV) of 43 000 h^{-1}. The CO oxidation was also performed over 1 mg of both fine Rh metal particles and Rh_2O_3 mixed with 200 mg of SiO_2 under the same experimental conditions, which is ∼3 times more than the Rh content present in 50 mg of 1% Rh/CeO_2 catalyst. To check for the stability of active rhodium species, the CO oxidation was carried out over heat-treated and reduced 1 atom % Rh/CeO_2 catalyst under stoichiometric condition when 2 vol % of CO and 1 vol % O_2 were used, keeping all other parameters unchanged. The sample temperature was monitored by a fine chromel−alumel thermocouple placed in the catalyst bed. The gas flow was controlled using mass flow sensors (Bronkhorst Hi-Tech BV and Honeywell AWM3100V) calibrated against standard bubble flow meter. Before the catalytic test, the as-prepared catalyst was heated at 200 °C for 30 min followed by degassing in He flow to the experimental temperature. All reactions were carried out as a function of temperature with a linear heating rate of 10° min^{-1} in a similar way as reported earlier.[13,20]

Results

Catalytic Test. Percentage CO conversion and CO_2 formation rates over Rh/CeO_2 catalysts as a function of temperature is presented in Figure 1a. The CO oxidation starts at ∼150 °C over the catalysts and complete CO conversion takes place at ∼220 °C. The light-off temperatures (50% conversion temperature, T_{50}) are 210 and 205 °C for 0.5 and 1% Rh/CeO_2, respectively. There is little change in T_{50} for 2% Rh/CeO_2 as compared to 1% Rh/CeO_2. Further, 0.5−1 atom % Rh over CeO_2 is sufficient to have a maximum catalytic effect. The figure also shows the percentage CO conversion over Rh metal particles, Rh_2O_3, and pure CeO_2 for comparison. Over Rh metal, CO oxidation begins at 215 °C and completes at 330 °C, and over Rh_2O_3, CO oxidation starts occurring at 275 °C and it completes at 485 °C. The T_{50} of the metal and oxide are 287 and 397 °C, respectively, indicating much lower activity compared to combustion-synthesized Rh/CeO_2 catalysts. An interesting point to note is that the activity of pure ceria is greater than that of Rh_2O_3 itself. In pure ceria, the CO oxidation starts at 230 °C and ends at 470 °C, the light off temperature being 355 °C. After each cycle the catalysts were cooled in oxygen flow to room temperature and subjected to a second cycle of CO oxidation and so forth. These repeated CO oxidation cycles over the same catalyst showed no change in activity. Figure 1b shows the CO oxidation activity of 1 atom % Rh/CeO_2 catalyst in two forms, one heated in air at 500 °C for 100 h and the other reduced in H_2 at 500 °C for 100 h, under stoichiometric conditions ($CO + {}^1/_2O_2$) . Clearly, one can see that the percent conversion is lower over the reduced catalyst than that of the oxidized catalyst. A drastic decrease of T_{50} from CeO_2 to Rh/CeO_2 and also in comparison with pure Rh metal, Rh_2O_3, and the reduced Rh/CeO_2 is to be attributed to the Rh−CeO_2 interaction in the as-synthesized Rh/CeO_2 catalyst.

Textural Study. The BET specific surface areas of the prepared catalyst samples are presented in Table 1. The surface area of the samples is in the range of 6−12 m^2/g. The average pore diameter of pure CeO_2 is ∼70 Å, which reduces to ∼60 Å in the catalyst samples. The adsorption/desorption isotherm (not shown) of pure CeO_2 is of type IV according to BDDT classification,[21] and the hysteresis loops are reduced to a great extent in the Rh/CeO_2 catalysts, indicating a great reduction of the pore system upon Rh incorporation.

H_2 Uptake. Figure 2 shows temperature-programmed reduction profiles for CeO_2, Rh_2O_3, and 0.5, 1, and 2% Rh/CeO_2. Pure CeO_2 shows H_2 uptake (oxygen storage capacity) above 200 °C and consisted of two peaks. The small first peak centered at ∼435 °C can be related to a global process corresponding to the consumption of surface oxygen species[22] and the redox process beyond 500 °C is to be attributed to bulk reduction. The total volume of hydrogen consumed is 8.2 cm^3 g^{-1} of CeO_2 up to 800 °C, which is equivalent to 4.1 cm^3 of O_2 g^{-1}. This corresponds to the reduction of CeO_2 to $CeO_{1.94}$. For the low surface area CeO_2 used here, the hydrogen uptake during the first peak is 61 μmol g^{-1} between 200 and 500 °C. In a recent study, Perrichon et al. have proposed a direct correlation between BET surface area and hydrogen uptake for CeO_2.[23] From their studies, for CeO_2 with a surface area of 12 m^2 g^{-1}, the H_2 uptake will be 39 μmol g^{-1} from the experimental curve and 55 μmol g^{-1} from the symmetrical peak procedure. According to the method proposed by Johnson and Mooi,[24] the expected value of H_2 uptake is 68 μmol g^{-1} for this CeO_2. Our observed value of 61 μmol g^{-1} agrees well with these studies.

Rh_2O_3 shows hydrogen uptake with a peak at 180 °C. The volume of H_2 calculated from the area under the peak corresponds to reduction of Rh_2O_3 to Rh metal according to the equation $Rh_2O_3 + 3H_2 \rightarrow 2Rh + 3H_2O$. The temperature at which H_2 uptake occurs over Rh/CeO_2 samples is between 30 and 125 °C, and reduction of the catalyst continues to occur with an increase in

(19) Bevington, P. R. In *Data Reduction and Error Analysis for Physical Sciences*; McGraw-Hill: New York, 1969.
(20) Bera, P.; Gayen, A.; Hegde, M. S.; Lalla, N. P.; Spadaro, L.; Frusteri, F.; Arena, F. *J. Phys. Chem. B* **2003**, *107*, 6122.
(21) Gregg, S. J.; Sing, K. S. W. In *Adsorption, Surface Area and Porosity*; Academic Press: London, 1991.
(22) Yao, H. C.; Yao, Y. F. *J. Catal.* **1984**, *86*, 254.
(23) Perrichon, V.; Laachir, A.; Bergeret, G.; Fréty, R.; Tournayan, L. *J. Chem. Soc., Faraday Soc.* **1994**, *90*(5), 773.
(24) Johnson, M. F. L.; Mooi, J. *J. Catal.* **1987**, *103*, 502; **1993**, *140*, 612.

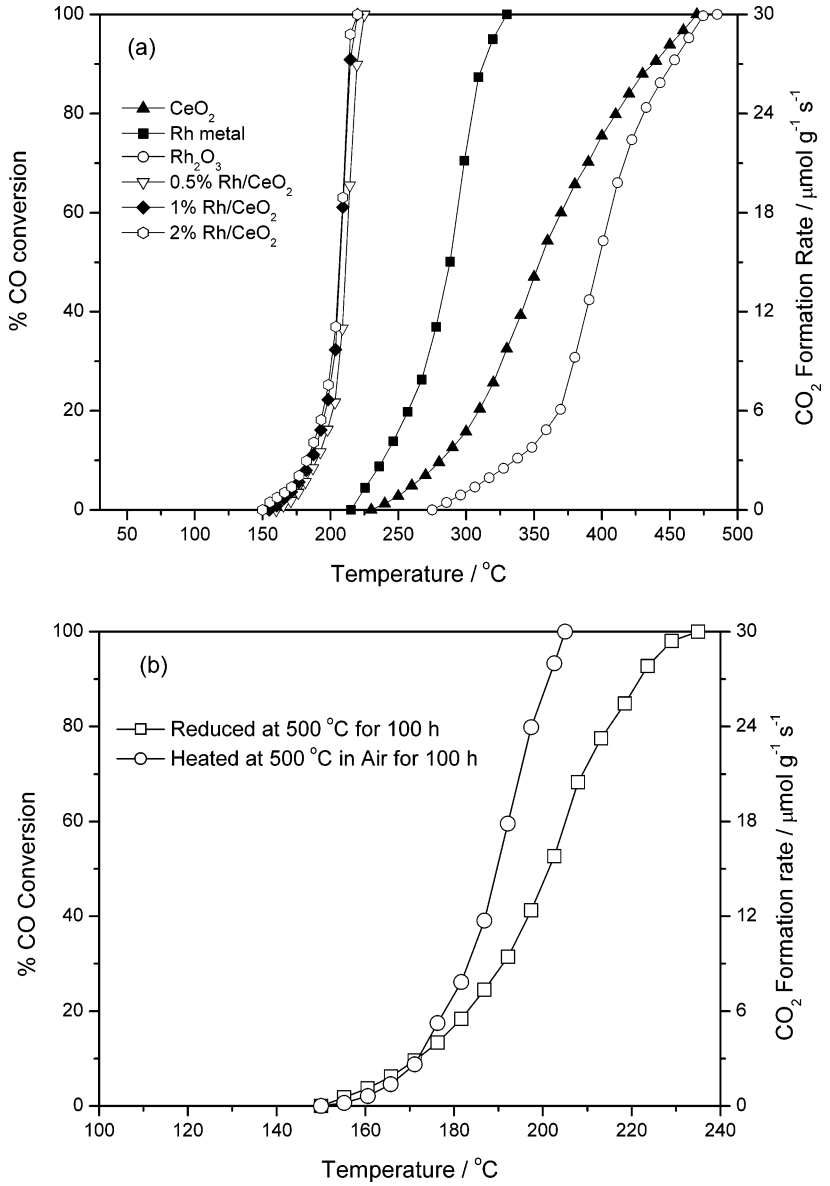

Figure 1. Percent CO conversion and corresponding rates for CO + O_2 reaction: (a) under excess oxygen over CeO_2, Rh metal, Rh_2O_3, 0.5% Rh/CeO_2, 1% Rh/CeO_2, and 2% Rh/CeO_2 and (b) under stoichiometric condition over air-heated and H_2-reduced 1 atom % Rh/CeO_2 at 500 °C for 100 h.

Table 1. Textural Properties of CeO_2 and Rh/CeO_2 Crystallites

catalyst	spec surf. area ($m^2\ g^{-1}$)	total pore vol ($cm^{-3}\ g^{-1}$)	av pore diameter (Å)
CeO_2	12	0.0211	72
0.5% Rh/CeO_2	6	0.0090	62
1% Rh/CeO_2	9	0.0139	62
2% Rh/CeO_2	10	0.0151	63

temperature. On the contrary, for pure Rh_2O_3, almost a flat background is obtained after peaking at ~180 °C, indicating no hydrogen consumption. For Rh/CeO_2 catalysts, the main peak at ~100 ± 10 °C can be attributed to the reduction of rhodium-associated species in the catalyst, and the second broad hump centered at ~270 °C corresponds to reduction of ceria, as is seen in the case of pure ceria. There are multiple H_2 reduction peaks at 55, 80, and 97 °C in 2% Rh/CeO_2, and they are to be attributed to different Rh sites in the CeO_2 matrix. The area under the main peak was computed and the hydrogen uptake values are 157, 141, and 244 μmol g^{-1} of the catalyst, respectively, for 0.5, 1, and 2 atom % Rh/CeO_2. Since this peak is related to Rh content in the catalyst, the H_2/Rh ratio was calculated and the respective values obtained are 5.4, 2.4, and 2.1. If the catalyst contained Rh_2O_3 phase, the H_2/Rh ratio should have been 1.5, as has been obtained for pure Rh_2O_3. Therefore, in Rh/CeO_2 catalyst, Rh_2O_3 is not present as an oxide phase. A high H_2/Rh ratio indicates that part of the CeO_2 gets reduced at lower temperature, effectively increasing the oxygen storage capacity of ceria at a lower temperature than pure CeO_2. As the Rh content is increased, the H_2/Rh ratio comes down. Thus, the hydrogen uptake study indeed shows that there is a chemical interaction between Rh and CeO_2 that is responsible for bring down the H_2 uptake temperature as well as the high H_2/Rh ratio.

XRD Studies. The X-ray diffraction patterns of the Rh/CeO_2 catalysts were recorded to check for the presence of rhodium metal or its oxide phases. The XRD patterns corresponded to the CeO_2 phase, and diffraction lines due to Rh_2O_3, RhO_2 and Rh metal could not

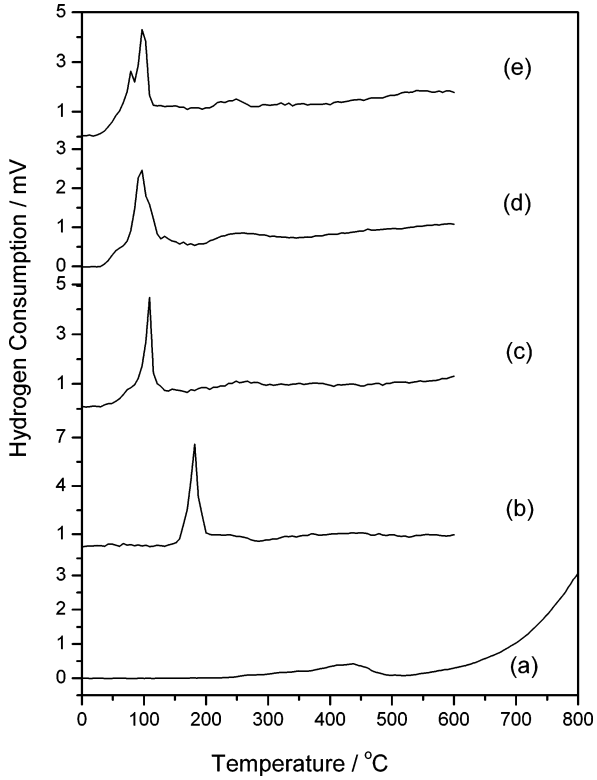

Figure 2. TPR profiles of (a) CeO_2, (b) Rh_2O_3, (c) 0.5% Rh/CeO_2, (d) 1% Rh/CeO_2, and (e) 2% Rh/CeO_2.

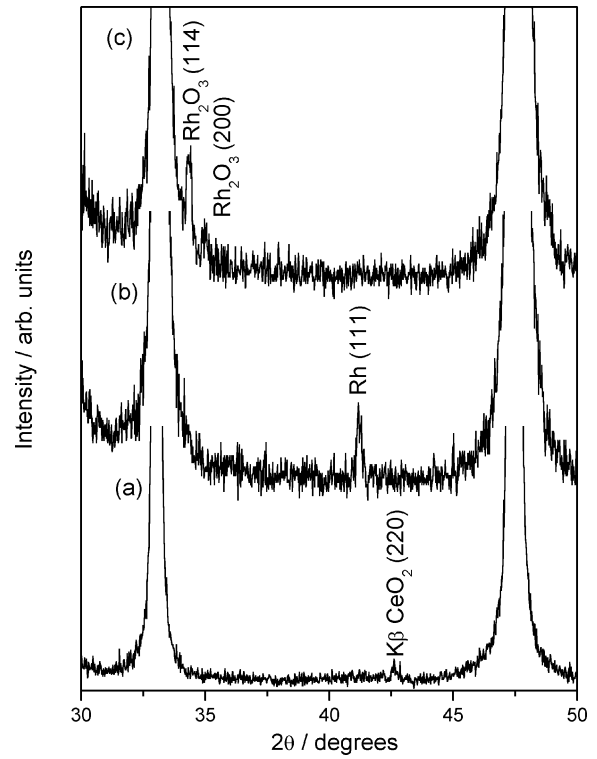

Figure 3. XRD patterns of (a) 1 atom % Rh/CeO_2, (b) 1 atom % Rh + CeO_2 (physical mixture), and (c) 1 atom % Rh_2O_3 + CeO_2 (physical mixture) in the range $2\theta = 30-50°$.

be detected. To confirm this further, 1 atom % Rh metal fine powder and 1 atom % Rh_2O_3 were physically mixed with the combustion-synthesized CeO_2 and XRD patterns were recorded. In Figure 3, we compare the XRD plots of 1 atom % Rh/CeO_2 prepared by combustion synthesis, 1 atom % Rh metal + CeO_2, and 1 atom % Rh_2O_3 + CeO_2 in the 2θ range of 30°−50° with a 40 times *y*-scale expansion. All the patterns were normalized with respect to the CeO_2(111) line at $2\theta = 28.6°$. Clearly one can see the Rh(111) peak and the Rh_2O_3(114) and (200) peaks in the physical mixtures. These reflections are absent in the combustion-synthesized Rh/CeO_2 catalyst. Therefore, the presence of Rh metal and Rh_2O_3 in the Rh/CeO_2 catalysts can be ruled out. Rh forms a stable Rh_2O_3 phase. Therefore, under the highly oxidizing preparation conditions, the $CeRhO_3$ phase is not expected. Also, diffraction lines due to $CeRhO_3$ as well as RhO_2 are not observed. Therefore, the possibility of Rh ion substitution for Ce^{4+} in the CeO_2 matrix was considered.

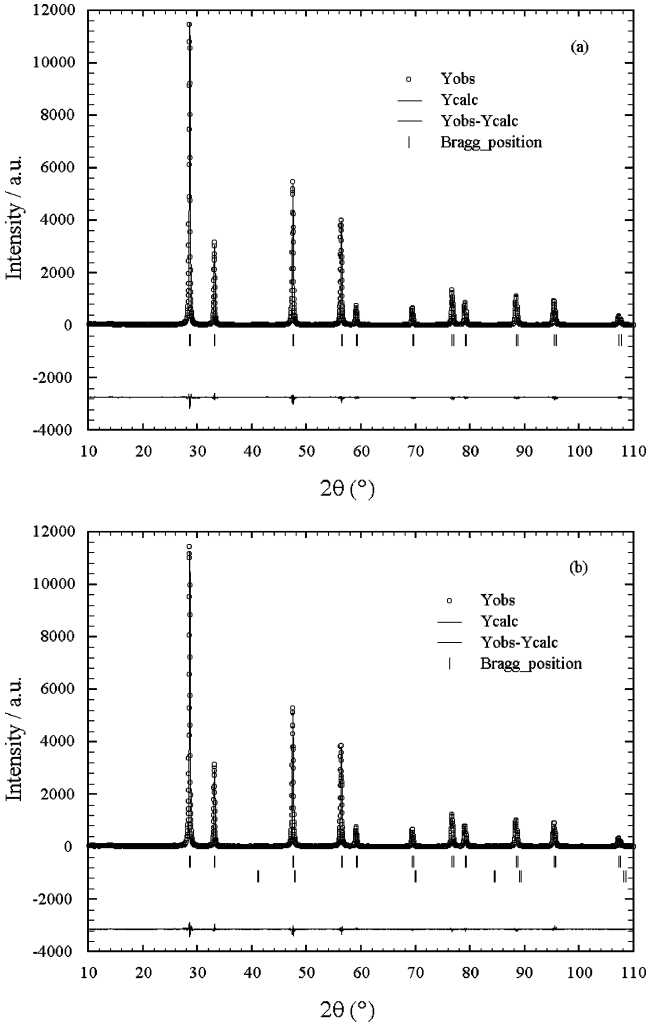

Figure 4. Observed, calculated, and difference XRD patterns of (a) 1% Rh/CeO_2 and (b) 2% Rh/CeO_2.

Rietveld analysis of 1 and 2 atom % Rh/CeO_2 XRD data was done using the program FullProf-fp2k. The total number of parameters varied was 19, such as overall scale factor, background parameters, unit cell, half width, shape, and isotropic thermal parameters along with oxygen occupancy. Rietveld refined patterns of 1 and 2 atom % Rh/CeO_2 are shown in Figure 4a and b, respectively. The diffraction lines are indexed to the fluorite structure ($Fm3m$). In 1 atom % Rh/CeO_2, the R_{Bragg}, R_F, and R_P values are 1.25, 0.853, and 5.5%, respectively. The lattice parameter a is 5.4109(1) Å. The R-factors R_{Bragg}, R_F, and R_P without Rh ion substituting for Ce^{4+} and refining only for CeO_2 are 1.3, 0.88, and

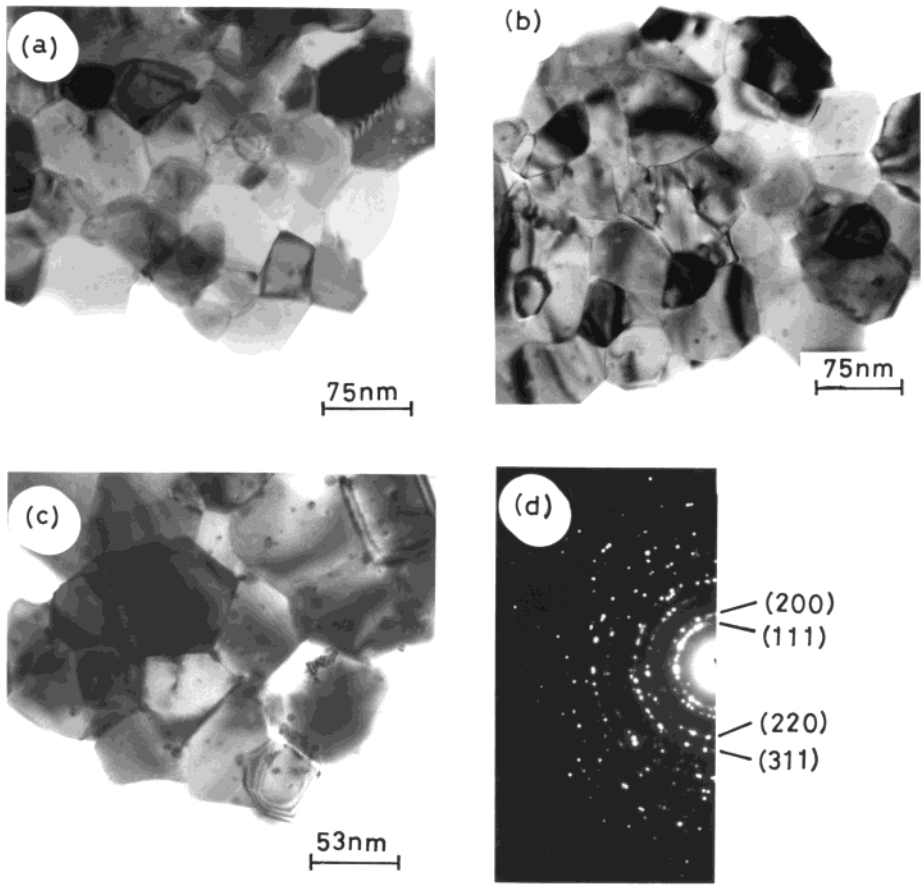

Figure 5. TEM image of (a) 0.5% Rh/CeO_2, (b) 1% Rh/CeO_2, and (c) 2% Rh/CeO_2 and (d) ED pattern of 1% Rh/CeO_2.

6.51%, respectively, which are higher than the refinement with Rh ion substitution. Hence, Rietveld refinement does indicate Rh ion substitution in the CeO_2 lattice. Pure CeO_2 was also refined, and R_{Bragg}, R_F, and R_P are 0.91, 0.70, and 4.4%, respectively. The a value for pure CeO_2 is 5.4113(3) Å. Total oxygen in 1 atom % Rh/CeO_2 is 1.87 and that in pure CeO_2 is 1.93. The quality of X-ray data is to be considered good from the excellent signal-to-noise ratio. The fitting is good as seen from R-factor values. Even though the X-ray scattering factor of oxygen is low compared to that of cerium, the absolute oxygen content obtained from the refinement can give us the trend in the variation of oxygen content. A decrease of oxygen content from 1.93 in pure CeO_2 to 1.87 in 1 atom % Rh/CeO_2 is significant. There is also a decrease in the lattice parameter in 1 atom % Rh/CeO_2 compared to pure CeO_2, but it is small. XRD of 0.5 atom % Rh/CeO_2 (not shown) has also been indexed to the fluorite structure without any impurity lines. The refined parameters are close to those of pure CeO_2. In the case of 2 atom % Rh/CeO_2, when the region around $2\theta = 41.15°$ is exploded, a small peak due to Rh(111) can be seen in the pattern, indicating the presence of a trace amount of Rh metal particles. Two-phase Rietveld refinement of this pattern gave the presence of about 1.2% Rh metal and 98.8% of Rh-substituted ceria phase. So out of 2 atom % Rh taken in the preparation, a negligible amount (1.2% of 2 atom %) separates as metal. This indicates that mostly rhodium ions are incorporated in the ceria matrix. The R_{Bragg}, R_F, and R_P values are 1.18, 0.925, and 6.2%, respectively. As has been shown, 0.5−1 atom % Rh is sufficient for high catalytic activity where Rh metal/metal clusters have not been detected. At 2 atom % Rh/CeO_2, observation of Rh metal even to a small extent suggests segregation of Rh ions to the surface of CeO_2 crystallites.

Rietveld refinement of 1 and 2 atom % Rh/CeO_2 gives a clear indication of Rh ion incorporation in the CeO_2 lattice. However, the changes in the lattice parameter are quite small. Rietveld refinement of the XRD pattern will not be an ideal tool to investigate if the Rh ions are dispersed in the surface layers and its local chemical environment. Hence TEM, XPS, and EXAFS studies were undertaken.

TEM Studies. TEM images of 0.5, 1, and 2 atom % Rh/CeO_2 and the electron diffraction (ED) pattern of 1 atom % Rh/CeO_2 are presented in Figure 5a−d. The average sizes of crystallites of CeO_2 are in the range of 50−60 nm. Well-defined edges of CeO_2 crystallites indicate the high crystallinity of CeO_2. The diffraction pattern obtained from these crystallites can be indexed to CeO_2 only (Figure 5d). There are a few dark patches in the image of <1 nm, indicating high electron density, and it may be due to Rh clusters. In 0.5% Rh/CeO_2, these dark patches are far and few, but there are white patches due to pits in the CeO_2.

To see growth of metal from Rh/CeO_2, the TEM of 1 atom % Rh/CeO_2 reduced in H_2 at 500 °C was taken, and in Figure 6a,b the TEM image and ED pattern are given. Here we can see Rh metal particles of 3−4 nm size over 50−60 nm CeO_2 crystallites. The study therefore shows that in 1 atom % Rh/CeO_2, Rh metal particles are far and few between but in hydrogen-reduced 1 atom % Rh/CeO_2, Rh metal particles of 3−4 nm can be

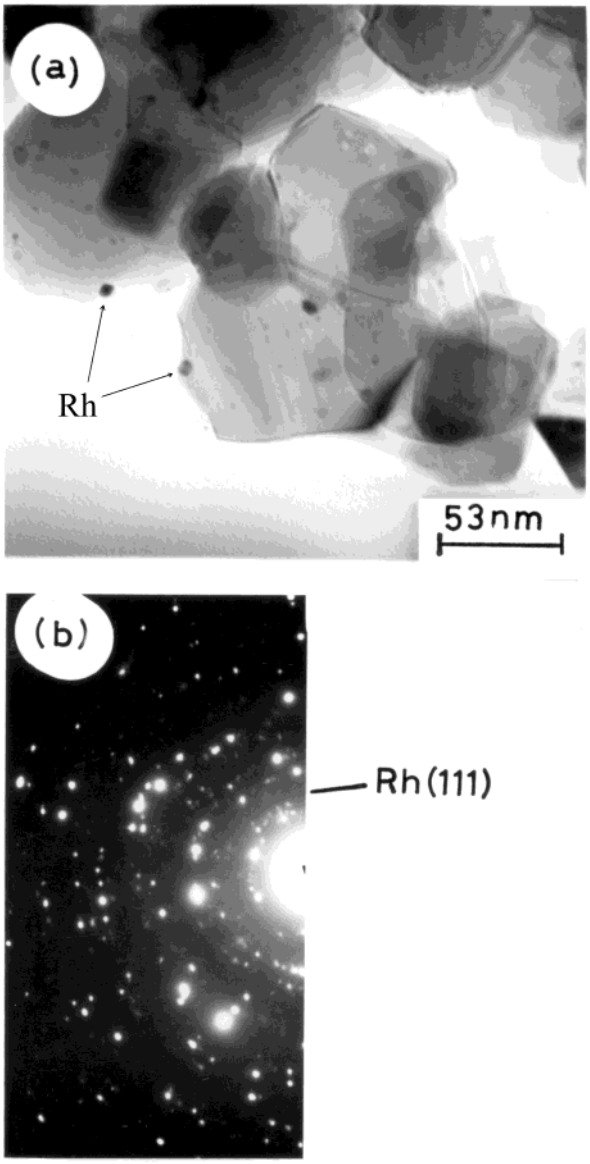

Figure 6. TEM (a) and ED pattern (b) of reduced 1% Rh/CeO_2.

observed. Thus, combustion-synthesized Rh/CeO_2 provides highly dispersed Rh in the CeO_2 matrix.

XPS Studies. Figure 7 shows the Rh(3d) core level region of Rh metal, Rh_2O_3, 1 and 2% Rh/CeO_2 catalysts. Accordingly, the $3d_{5/2,3/2}$ doublet at 307.2, 312.0 is due to Rh metal in the zerovalent state. In Rh_2O_3, 308.8, 313.6 eV peaks are due to rhodium in the +3 oxidation state.[25,26] The Rh(3d) core level region of 1 and 2 atom % Rh/CeO_2 shows three major peaks. The first peak in both the spectra at the lower binding energy side at ~303.3 eV is due to the Ce(M_3VV) Auger line. The second and third peak at 308.8 and 313.6 eV can be assigned to the $3d_{5/2,3/2}$ doublet of Rh in the +3 oxidation state. Unlike in the Rh metal and Rh_2O_3, the Rh(3d) peaks in Rh/CeO_2 samples are broad. Since there is no clear indication of splitting of the $3d_{5/2}$ peak, it is difficult to resolve it into mixed-valent Rh in Rh/CeO_2. XPS of

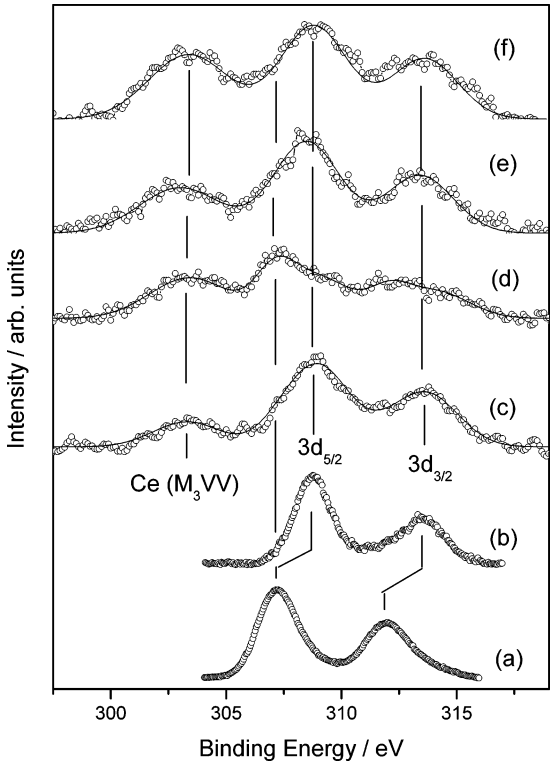

Figure 7. Rh(3d) core level region of (a) Rh metal, (b) Rh_2O_3, (c) 1% Rh/CeO_2 (as-prepared), (d) 1% Rh/CeO_2 (reduced in H_2 at 500 °C for 100 h), (e) 1% Rh/CeO_2 (air-heated at 500 °C for 100 h), and (f) 2% Rh/CeO_2.

0.5 atom % Rh/CeO_2 was also recorded, and it did show the presence of Rh^{3+}. Upon reduction of 1 atom % Rh/CeO_2 in pure H_2 at 500 °C for 100 h, Rh(3d) spectra shows the presence of Rh in the 0 and +3 state (Figure 7, curve d). The air-heated sample at 500 °C shows only the oxidized Rh in the +3 state (curve e). In 2 atom % Rh/CeO_2, also Rh is present in the +3 state (curve f).

Figure 8 shows the Ce(3d) core level region of as-prepared, reduced, and heat-treated 1 atom % Rh/CeO_2 and 2 atom % Rh/CeO_2. Thus, Ce($3d_{5/2,3/2}$) peaks at 882.9 and 901.3 eV with satellite features (marked in the figure) correspond to CeO_2 with Ce in the +4 oxidation state.[27] As can be seen from the figure, reduction of Ce^{4+} to Ce^{3+} is not significant in the H_2 reduced sample from the relative intensities of the main Ce(3d) and satellite peaks (compare curves a and b). Although the H_2 uptake study certainly indicates reduction of Ce^{4+} to Ce^{3+}, XPS is not sensitive enough to find this. It is also possible that while transferring the sample to the XPS chamber in air, oxidation of Ce^{3+} could have occurred.

The surface concentration of Rh calculated from the intensity ratios employing the methodology of Powell and Larson[28] comes out to be 3.6% for 1% Rh/CeO_2 and 3.3% for 2 atom % Rh/CeO_2. Photoionization cross sections and mean free path of the photoelectrons were obtained from Scotfield[29] and Penn,[30] respectively. Thus, the surface Rh concentration is about 3.5 times higher than the bulk concentration in 1% $RhCeO_2$. The maximum surface enrichment takes place at the 1 atom %

(25) Katzer, J. R.; Sleight, A. W.; Gajardo, P.; Michel, J. B.; Gleason, E. F.; McMillan, S. T. *Faraday Discuss. Chem. Soc.* **1981**, *72*, 121.
(26) Kawai, M.; Uda, M.; Ichikawa, M. *J. Phys. Chem.* **1985**, *89*, 1654.
(27) Sarma, D. D.; Hegde, M. S.; Rao, C. N. R. *J. Chem. Soc., Faraday Trans. 2* **1981**, *77*, 1509.
(28) Powell, C. J.; Larson, P. E. *Appl. Surf. Sci.* **1978**, *1*, 186.
(29) Scotfield, J. H. *J. Electron Spec. Relat. Phenom.* **1976**, *8*, 129.
(30) Penn, D. R. *J. Electron Spec. Relat. Phenom.* **1976**, *9*, 29.

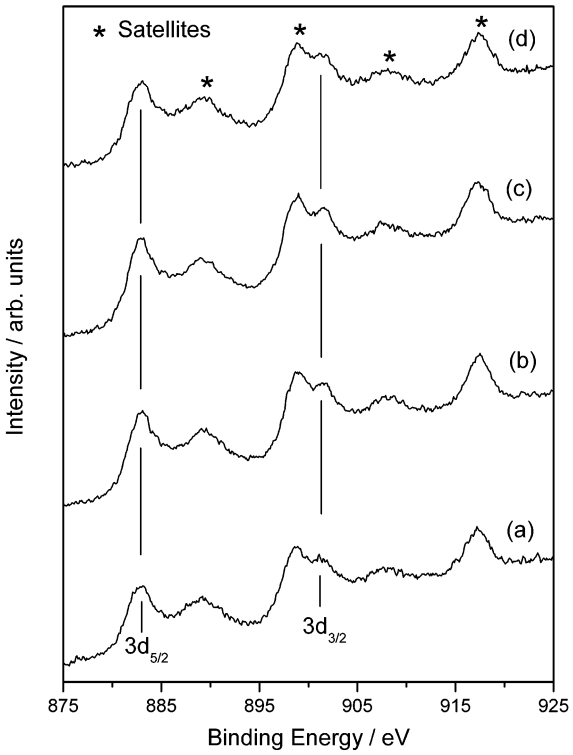

Figure 8. XPS of Ce(3d) region in (a) 1% Rh/CeO_2 (as-prepared), (b) 1% Rh/CeO_2 (reduced in H_2 at 500 °C for 100 h), (c) 1% Rh/CeO_2 (air-heated at 500 °C for 100 h), and (d) 2% Rh/CeO_2.

doping level, beyond which the Rh either goes to the bulk or part of it separates as tiny metal particles. On heat-treatment, the surface concentration of Rh in 1 atom % Rh/CeO_2 remains essentially unaltered (3.4%), but it is decreased to 2.4% in reduced 1 atom % Rh/CeO_2.

XRD, TEM, and XPS studies indicate that Rh is ionically dispersed over CeO_2 support in the combustion-synthesized catalysts. Low-temperature CO oxidation, H_2 uptake studies indicate a chemical interaction between dispersed Rh ions and CeO_2. However, these studies do not provide the local environment of the Rh ions. To probe the local structure of Rh in these catalysts, EXAFS studies at the Rh K-edge of Rh/CeO_2 catalysts have been carried out.

EXAFS Studies. The normalized XANES spectra of model compounds, Rh metal, Rh_2O_3, and the catalyst samples are presented in Figure 9. The edge energy, as determined from the first maxima in the derivative spectra, for Rh metal is found to be 23 219.0 eV. It is shifted to 23 228.0 eV for Rh_2O_3. The near-edge structure, which is a signature of the local environment around the absorbing atom, also shows clear differences in the case of the two model compounds. The Rh atom in Rh metal is surrounded by 12 other Rh atoms, forming a cubooctahedron, while in the case of Rh_2O_3, Rh is coordinated to six oxygens in a rhombohedral structure.[31] In the case of catalyst samples, the value of edge energy was found to be around 23 228.0 eV, indicating the presence of Rh in the ionic phase. Furthermore, the near-edge structure in these two

(31) Grier, D.; McCarthy, G. ICDD Grant-in-Aid 1991, PDF # 431025.

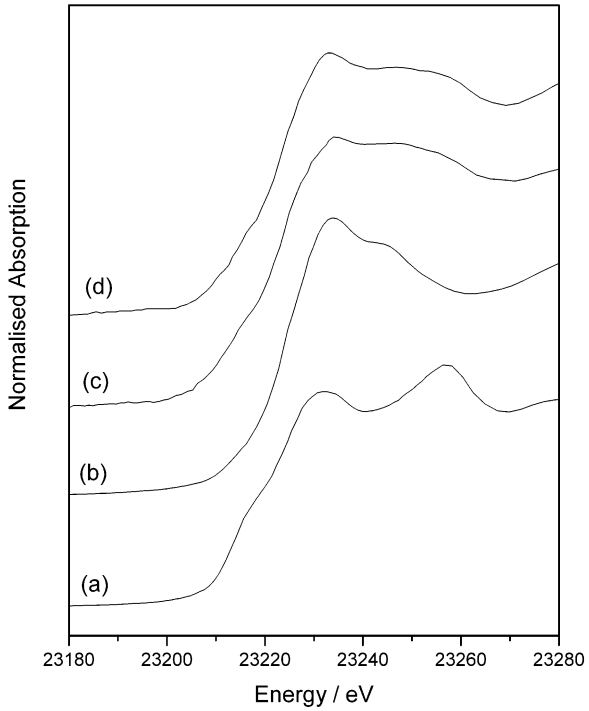

Figure 9. Normalized XANES spectra at the Rh K-edge of (a) Rh metal, (b) Rh_2O_3, (c) 1% Rh/CeO_2, and (d) 2% Rh/CeO_2.

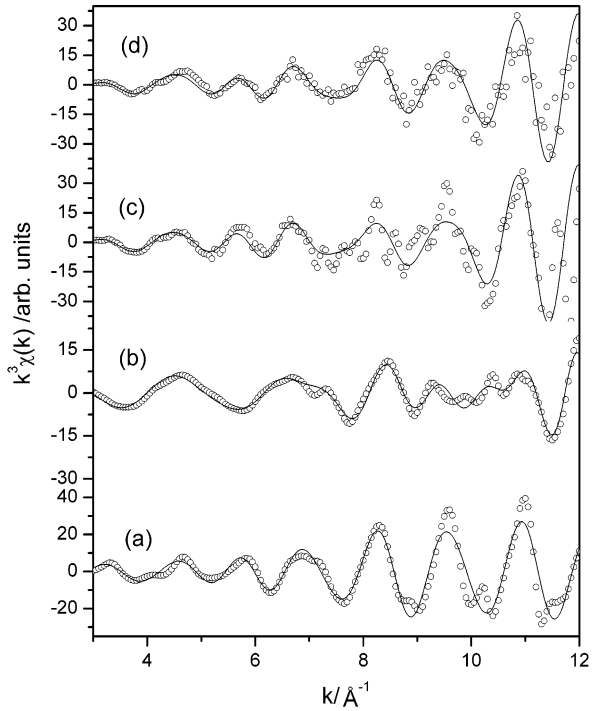

Figure 10. k^3-Weighted EXAFS functions of (a) Rh metal, (b) Rh_2O_3, (c) 1% Rh/CeO_2, and (d) 2% Rh/CeO_2 along with fitted curves shown as a solid line.

samples is also completely different from that in Rh metal or Rh_2O_3. Even in the case of 0.5% Rh/CeO_2, the Rh K-edge was shifted by 9 eV with respect to metal, indicating Rh to be in an ionic state. However, due to a poor signal-to-noise ratio, the data was not used for further analysis.

The normalized, k^3-weighted EXAFS spectra of Rh metal, Rh_2O_3, and the catalysts are presented in Figure 10. The EXAFS spectra of both the catalyst samples are different from that of Rh metal and Rh_2O_3 in terms of

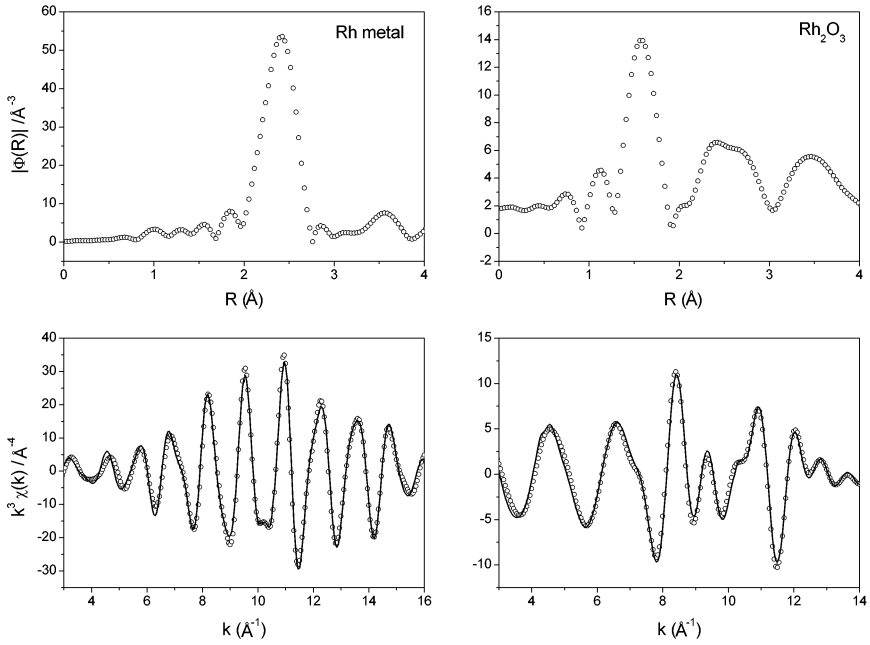

Figure 11. Fourier transforms and inverse transforms of Rh metal and Rh_2O_3.

Table 2. Structural Parameters of Rh Metal and Rh_2O_3 Obtained from EXAFS Analysis

samples	shell	N	R (Å)	σ^2 (Å^{-2})
Rh	Rh−Rh	12.00	2.687 ± 0.002	0.004 ± 0.001
		6.00	3.800 ± 0.003	0.006 ± 0.001
		48.00	4.030 ± 0.003	0.005 ± 0.002
		24.00	4.653 ± 0.004	0.006 ± 0.002
Rh_2O_3	Rh−O	5.6 ± 0.4	2.026 ± 0.004	0.003 ± 0.001
	Rh−Rh	1.0 ± 0.3	2.682 ± 0.002	0.004 ± 0.001
	Rh−Rh	3.0 ± 0.6	3.030 ± 0.006	0.007 ± 0.003
	Rh−O	2.8 ± 0.4	3.410 ± 0.006	0.002 ± 0.001
	Rh−Rh	2.9 ± 0.4	3.520 ± 0.006	0.013 ± 0.008

frequency maxima positions. Data only up to 12 Å^{-1} have been used for analysis due to a poor signal-to-noise ratio at higher k values.

Figure 11 shows the k^3-weighted Fourier transform (FT) of the EXAFS spectra for Rh metal and Rh_2O_3 along with their inverse transforms. The Fourier transforms are not corrected for phase shift, and hence, the peaks are shifted to lower R values. The values of bond distance quoted in the text and table are, however, corrected for phase shift. For Rh metal, the first Rh−Rh scattering peak is seen at 2.68 Å, which has a coordination number of 12, as expected for face-centered cubic Rh metal. The structural parameters obtained from the fitting are presented in Table 2. In the FT of Rh_2O_3, the first peak at 1.6 Å in the figure corresponds to Rh−O correlations at 2.02 and 2.04 Å in Rh_2O_3. The second broad peak corresponds to Rh−Rh scattering with bond distances of 2.68 and 3.03 Å. The values of bond distance, coordination number, and Debye−Waller factors obtained from fitting the EXAFS data in the R range from 1 to 4 Å are presented in Table 2. These values agree well with the structural data of Rh and Rh_2O_3.[15,31]

EXAFS data of Rh/CeO_2 catalysts were fitted with several structural models, such as Rh metal, Rh_2O_3 phases dispersed on CeO_2, RhO-like($a \sim 4.13$ Å) layer over CeO_2 ($a \sim 5.411$ Å), and the solid solution model with Rh ion substituting for Ce^{4+} ion in CeO_2, i.e., $Ce_{1-x}Rh_xO_{2-\delta}$. Fitting with the first three models was very poor. The k^3-weighted FT and inverse transform spectra of 1% Rh/CeO_2 and 2% Rh/CeO_2 catalysts fitted with solid solution model are presented in Figure 12. The fit is reasonably good. As above, the FT spectra are not corrected for phase shift, but the values in the text and the tables are phase-corrected. In both of these samples, a correlation at about 2.05 Å is seen, which agrees closely with the Rh−O bond length (correlation) in Rh_2O_3 at 2.03 Å. The second correlation at 2.72 Å can be attributed to Rh−Rh scattering, as this closely matches with the first near neighbor of Rh metal as well as the second near neighbor distance in Rh_2O_3. The third peak at 3.16 Å is however absent in both Rh metal as well as Rh_2O_3. With Rh ion in the Ce site of CeO_2, 3.16 Å should correspond to a Rh−O−Ce correlation. The fitted parameters obtained for the catalysts are listed in Table 3. In the solid solution phase, Rh has about 2.5 oxygen atoms in the first coordination. If Rh ions are substituted for Ce^{4+} sites, the first coordination around Rh ion will be of oxide ions. In the case of pure CeO_2, Ce^{4+} ions have eight oxide ion neighbors in bulk solid, but the surface Ce^{4+} ions will have only four O^{2-} ions. It is quite possible that Rh ions substituted for Ce^{4+} sites are largely in the surface layers of CeO_2 crystallites. In such a model, Rh ions should have four O^{2-} ions as neighbors in the first shell. Since Rh is in the +3 state, charge balance would require oxide ion vacancies around Rh ions. The lower coordination number (∼2.5) obtained for Rh−O correlation at 2.05 Å shows the presence of oxide ion vacancies around the Rh ion. Further, the substituted Rh ion will have correlations from Ce^{4+} ion as well as Rh in the second coordination. Because of the different sizes of the Rh ion and Ce^{4+} ion and also the ionic interaction between them, Rh−Rh and Rh−Ce correlations would appear as two separate correlations. Accordingly, the bond distances at 2.72 and 3.16 Å can be attributed to Rh−Rh and Rh−Ce correlations.

The total coordination number of ∼9 obtained for Rh−Rh and Rh−Ce correlation is higher than the second shell coordination of 8 for Ce^{4+} ions on the surface and

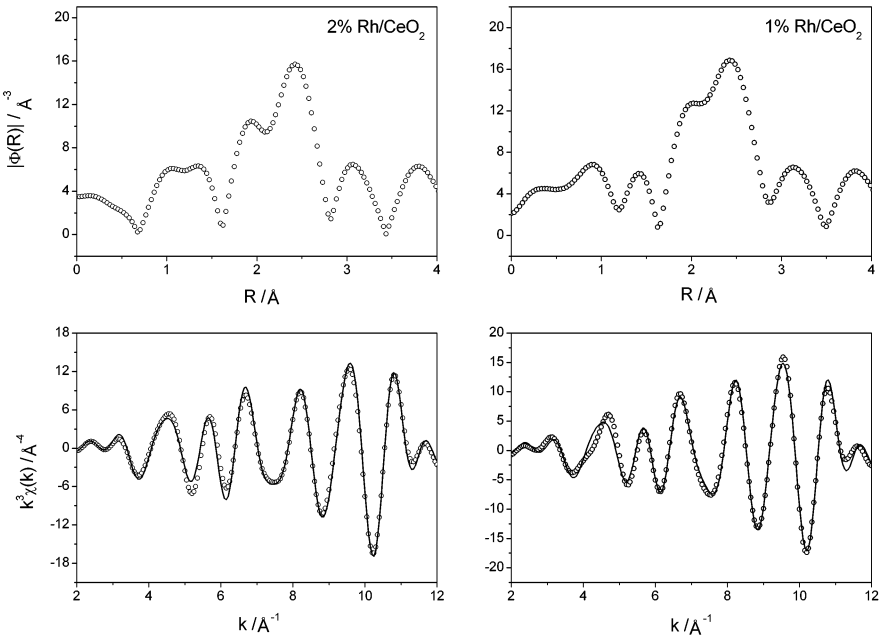

Figure 12. Fourier transforms and inverse transforms of 1 and 2% Rh/CeO_2.

Table 3. Structural Parameters for Rh/CeO_2 Catalysts Obtained from EXAFS Analysis

catalysts	shell	N	R (Å)	σ^2 (Å^{-2})
1% Rh/CeO_2	Rh−O	2.4 ± 0.6	2.045 ± 0.003	0.005 ± 0.001
	Rh−Rh	5.7 ± 0.3	2.722 ± 0.003	0.002 ± 0.001
	Rh−Ce	3.9 ± 0.4	3.163 ± 0.004	0.002 ± 0.001
2% Rh/CeO_2	Rh−O	2.3 ± 0.4	2.060 ± 0.005	0.007 ± 0.002
	Rh−Rh	5.4 ± 0.5	2.733 ± 0.003	0.002 ± 0.001
	Rh−Ce	5.1 ± 0.5	3.157 ± 0.006	0.002 ± 0.001

Table 4. Structural Parameters Obtained from EXAFS Analysis Using Solid Solution and Rh Metal Correlations

catalysts	shell	N	R (Å)	σ^2 (Å^{-2})
1% Rh/CeO_2	Rh−O	2.2 ± 0.6	2.049 ± 0.003	0.005 ± 0.002
	Rh−Rh	3.6 ± 0.4	2.754 ± 0.006	0.002 ± 0.001
	Rh−Ce	5.4 ± 0.7	3.214 ± 0.010	0.002 ± 0.003
	Rh−Rh[a]	3.9 ± 0.4	2.688 ± 0.004	0.004 ± 0.002
2% Rh/CeO_2	Rh−O	2.2 ± 0.6	2.091 ± 0.006	0.007 ± 0.003
	Rh−Rh	3.9 ± 0.6	2.759 ± 0.007	0.002 ± 0.001
	Rh−Ce	7.7 ± 0.9	3.202 ± 0.010	0.002 ± 0.004
	Rh−Rh[a]	3.9 ± 0.4	2.691 ± 0.004	0.004 ± 0.002

[a] From the first Rh−Rh correlation of small Rh metal particles.

lower than 12 for Ce^{4+} ions in the bulk CeO_2. In a similar study of 1 atom % Pd/CeO_2, $Pd^{2+}-O^{2-}$, $Pd^{2+}-Pd^{2+}$, and $Pd^{2+}-O^{2-}-Ce^{4+}$ correlations were observed at 2.02, 2.71, and 3.31 Å with coordination numbers 2.7 (O), 3.2 (Pd), and 7.3 (Ce).[11] A lower value of Rh−O−Ce correlation at 3.16 Å is to be expected, because Rh is in the +3 state. From the data in Table 3, a coordination number of ∼5.7 Rh in the second shell seems a bit higher for 1 atom % Rh/CeO_2.

To see if fitting can be improved and the higher Rh−Rh coordination number can be accounted for, the EXAFS data were fitted with a model containing Rh ion in the solid solution phase, $Ce_{1-x}Rh_xO_{2-\delta}$, along with Rh metal, since Rh−Rh correlation at 2.72 Å in Rh/CeO_2 catalysts is close to the Rh−Rh correlation at 2.68 Å in Rh metal itself. The structural parameters obtained from this analysis are presented in Table 4. The fitting is comparable with that obtained with only the solid solution model, and a lower Rh−Rh coordination of 3.6 is obtained in this fitting. But the R factors were higher for the (Rh + $Ce_{1-x}Rh_xO_{2-\delta}$) model than the $Ce_{1-x}Rh_xO_{2-\delta}$ model (0.045 vs 0.028 for 1 atom % Rh/CeO_2 and 0.06 vs 0.04 for 2 atom % Rh/CeO_2 for the two models, respectively). Therefore, substitution of Rh^{3+} ion in the form of $Ce_{1-x}Rh_xO_{2-\delta}$ seems to be reasonable from the fitting of the EXAFS data with specific Rh−O and Rh−O−Ce correlation at 2.03 and 3.16 Å, respectively.

Discussion

In the present study, we have carried out systematic structural investigations on combustion-synthesized Rh/CeO_2 catalysts. It has been an endeavor of researchers to reduce the amount of noble metal content without adversely affecting their catalytic properties. Ionic dispersion is an effective way to achieve this. Combustion synthesis provides in a single step ionically dispersed metal on ceria support.

The structure of 0.5−1 atom % Rh/CeO_2 is important, because the maximum Rh loading required is less than 1 atom %. To see how the Rh-related phases evolve with increase in Rh loading, 2 atom% Rh/CeO_2 was studied. The XRD pattern of 1% Rh/CeO_2 clearly ruled out Rh metal or Rh oxide phases. In the combustion-synthesized Rh/CeO_2, Rh ion taken in the preparation should be separated either into Rh metal particles or its oxides or Rh ion should be incorporated in the CeO_2 matrix. In the preparation, the Rh precursor taken is in the +3 state and Ce^{4+} and Rh^{3+} are totally mixed in the ionic state. The combustion of the precursor leading to a flame in the oxidizing atmosphere (air) lasts only for a few seconds. Thus, the high-temperature phase formed is quenched to form the active catalyst. In such a short period of time, separation of Rh ions in the form of Rh_2O_3 or reduction into Rh metal particles does not seem to occur. However, with an increase in Rh metal concentration (2 atom % Rh) an extremely small amount of Rh metal particles is separated, not Rh_2O_3. If Rh^{3+} substitutes for Ce^{4+} in the CeO_2 lattice, then charge neutrality demands oxide ion vacancies surrounding the Rh ion.

In 0.5 and 1 atom % Rh/CeO_2, Rh is fully in the oxidized state, which is the real catalyst. The CO oxidation study has demonstrated that even 0.5 atom % Rh is sufficient to effect high catalytic activity. Therefore, Rh ion dispersed in CeO_2 matrix is indeed the active site for $CO + O_2$ oxidation. Also, air-heated 1 atom % Rh/CeO_2 showed higher catalytic activity compared to the reduced catalyst. The higher surface concentration of Rh in the heat-treated catalyst compared to the reduced catalyst is in conformity with this observation, indicating oxidized Rh in CeO_2 as the active site for CO oxidation.

The hydrogen uptake measurement demonstrated the unique interaction of Rh and CeO_2 in terms of the decrease in reduction temperature from 180 °C in pure Rh_2O_3 to 100 ± 10 °C in Rh/CeO_2 catalysts. The oxygen storage capacity of Rh-substituted CeO_2 is higher than that of pure CeO_2, that too at much lower temperature. An H_2/Rh ratio of 5.4, 2.4, 2.1, respectively, for 0.5, 1, and 2% Rh/CeO_2 can definitely be attributed to contribution from the reduction of ceria at lower temperature, indicating a strong interaction between Rh and ceria.[32−34] This is to be expected, since oxide ion is bonded to both Rh^{3+} and Ce^{4+} ions in the solid solution model and reduction of Ce^{4+} to Ce^{3+} should occur to have a higher H_2/Rh ratio. The observed reduction temperature over combustion-synthesized Rh/CeO_2 is lower by ∼65 °C than the reported value by Fornasiero et al.[34] over 0.5 wt % Rh/CeO_2 prepared by the incipient wet impregnation method. The H_2 consumption temperature of 167 °C obtained by them is close to the Rh_2O_3 reduction temperature, suggesting the presence of oxidized rhodium in their catalyst.[34]

EXAFS studies show that Rh ions substitute for Ce^{4+} ions primarily on the surface in the form of $Ce_{1-x}Rh_xO_{2-\delta}$ solid solution. The enhanced surface concentration of Rh^{3+} in XPS indeed supports this point. In pure CeO_2, the $Ce^{4+}-O-Ce^{4+}$ correlation at 3.82 Å is due to Ce−O−Ce angle of 109.5°. Due to substitution of the smaller Rh^{3+} ion, geometry around the Rh^{3+} ion will be different from Ce^{4+} in CeO_2. Assuming an ionic radii of Rh^{3+} (0.665 Å), O^{2-} (1.4 Å), and Ce^{4+} (1.01 Å),[35] for the Rh−Ce distance of 3.16 Å the $Rh^{3+}-O-Ce^{4+}$ angle would be ∼95°. Similar correlations have been found by us in our earlier studies for Pd/CeO_2, Cu/CeO_2, and Pt/CeO_2 systems at 3.31, 3.15, and 3.28 Å, respectively, in the form of $Ce_{1-x}M_xO_{2-\delta}$ (M = Pd, Cu, and Pt) solid solution phase.[11−13]

Detailed structural and redox studies showed that in the combustion-synthesized Rh/CeO_2, $Rh-CeO_2$ interaction is in the form of $Ce_{1-x}Rh_xO_{2-\delta}$, mostly on the surface layers of CeO_2. Since Rh is present in the +3 state in combustion-synthesized Rh/CeO_2, Rh^{3+} ions should be the active sites for CO adsorption in the $CO + O_2$ reaction. For a higher rate of CO conversion at a lower temperature in the combustion-synthesized Rh/CeO_2, a higher amount of CO adsorption and availability of dissociated oxygen are essential. While Rh^{3+} ions can act as CO adsorption sites, additional oxygen adsorption sites would help achieve higher rates. Oxide ion vacancy, as demonstrated from both XRD and EXAFS studies, would be the natural oxygen adsorption sites next to Rh^{3+} ion sites. Therefore, lower temperature $CO + O_2$ reaction over combustion-synthesized Rh/CeO_2 is attributed to $Rh-CeO_2$ interaction in the form of $Ce_{1-x}Rh_xO_{2-\delta}$ solid solution having $-\square-Rh^{3+}-O-Ce^{4+}-O-$ site distribution in the surface layers of the catalyst crystallites. Based on this $Ce_{1-x}Rh_xO_{2-\delta}$ model, we propose following redox mechanism for CO oxidation by O_2.

$$^3/_2O_2 + 3\square_{O^{2-}}^{\bullet\bullet} \rightarrow 3O_o^x + 6h^\bullet$$

$$3(-Ce^{4+}-O-Rh^{3+}-) + 3CO + 3O_o^x \rightarrow 3(-Ce^{4+}-O-Rh^0-) + 3\square_{O^{2-}}^{\bullet\bullet} + 3CO_2\uparrow$$

$$3(-Ce^{4+}-O-Rh^0-) + 3h^\bullet \rightarrow 3(-Ce^{3+}-O-Rh^{3+}-)$$

$$3(-Ce^{3+}-O-Rh^{3+}-) + 3h^\bullet \rightarrow 3(-Ce^{4+}-O-Rh^{3+}-)$$

$$^3/_2O_2 + 3CO \rightarrow 3CO_2$$

In the above mechanism, one Rh^{3+} ion is reducing to Rh^0, and conversion of Rh^0 to Rh^{3+} via the holes ($h^\bullet$) created seems to reduce three Ce^{4+} to Ce^{3+}. That Rh ion is going from 3+ to 0 and partial reduction of Ce^{4+} to Ce^{3+} are supported from TPR experiments with a H_2/Rh ratio of more than what is needed to balance this equation. The oxygen vacancies ($\square_{O^{2-}}^{\bullet\bullet}$) seem to play a crucial role in the redox mechanism, and indeed both XRD and EXAFS has shown the presence of oxide ion vacancies. In the case of Cu/CeO_2, Pd/CeO_2, and Pt/CeO_2, metal ion seems to go from +2 to 0 and correspondingly only two Ce ions gets reduced.[10−12] Therefore, the lower concentration of Rh sufficient to bring about catalytic conversion supports the above mechanism.

The effect of addition of CeO_2 and PMs in terms of higher catalytic activity (decrease in reaction temperature and higher rate of conversion) has been known for a long time, and it was generally attributed to strong metal−support interaction. From this study, the actual interaction of Rh and CeO_2 is shown to be ionic−that is, substitution of metal ion for Ce^{4+} ion in the reducible CeO_2 support. The stabilization of Rh in ionic form over CeO_2 certainly hinders sintering into Rh metal particles. Our study therefore explains the qualitative description in catalysis literature, namely, high dispersion, higher oxygen storage capacity, higher catalytic activity, and strong metal−support interaction of Rh/CeO_2 system.

Conclusions

(a) Rh dispersed in an ionic state over 50 nm CeO_2 crystallites has been synthesized by the combustion technique.

(32) Trovarelli, A.; Dolcetti, G.; Leitenburg de C.; Kaŝpar; Finetti, P.; Santoni, A. *J. Chem. Soc., Faraday Trans.* **1992**, *88*(9), 1311.

(33) Rao, G. R.; Fornasiero, P.; Di Monte, R.; Kašper. J.; Vlaic, G.; Balducci, G.; Meriani, S.; Gubitosa, G.; Cremona, A. and Graziani, M. *J. Catal.* **1996**, *162*, 1.

(34) Fornasiero, P.; Kašper, J.; Graziani, M. *J. Catal.* **1997**, *167*, 576.

(35) Dickinson, S. K., Jr. In *Ionic, Covalent and Metallic Radii of the Chemical Elements*; Airforce Cambridge Research Laboratories: L. G. Hanscom Field, Bedford, MA, 1970.

(b) In comparison to Rh metal and Rh_2O_3, the Rh ions dispersed over CeO_2 are more active for CO oxidation.

(c) H_2/Rh ratio of 5.4, 2.4, and 2.1, respectively, for 0.5, 1, and 2% Rh/CeO_2 suggests sufficiently high contribution from ceria reduction at lower temperature.

(d) Rietveld refinement confirms the absence of rhodium metal or rhodium oxide phases.

(e) TEM study shows absence of Rh metal particles in 0.5 and 1 atom % Rh/CeO_2 catalyst.

(f) XPS and XANES studies of catalysts show that Rh is present in the ionic state.

(g) EXAFS analysis shows that Rh ion is substituted for Ce^{4+} ion in the surface layers of CeO_2 crystallites with oxide ion vacancies around it.

(h) A $Rh^{3+}-O-Ce^{4+}$ correlation at 3.16 Å in Rh/CeO_2 catalysts has been shown from EXAFS analysis.

(i) The metal−ceria interaction in the form of $Ce_{1-x}Rh_xO_{2-\delta}$ solid solution mostly in the surface layers of CeO_2 crystallites is responsible for enhanced catalytic activity.

Acknowledgment. The authors gratefully acknowledge financial support from the Department of Science and Technology (DST), Government of India. Thanks are due to Japan Synchrotron Radiation Research Institute (SPring-8), for allotting beamtime at BL01B1 beamline (Proposal No. 2003A0028-Cx-np). We thank Dr. N. P. Lalla, IUC, Indore, for recording XRD data. A.G. is thankful to the Council of Scientific and Industrial Research (CSIR), Government of India, for the award of a research fellowship. Thanks are due to C. R. Reddy and B. V. Kumar, Bangalore Institute of Technology, for surface area measurement. K.R.P. thanks the Indian Academy of Sciences for the award of a Summer Research Fellowship.

CM040126L